analytical chemistry

pubs.acs.org/ac Article

Analysis of the Stable Isotope Ratios ($^{18}O/^{16}O$, $^{17}O/^{16}O$, and D/H) in Glacier Water by Laser Spectrometry

Xiaojuan Cui,* Weidong Chen, Markus Werner Sigrist, Eric Fertein, Pascal Flament, Kevin De Bondt, and Nadine Mattielli

Cite This: *Anal. Chem.* 2020, 92, 4512−4517 Read Online

ACCESS | Metrics & More | Article Recommendations

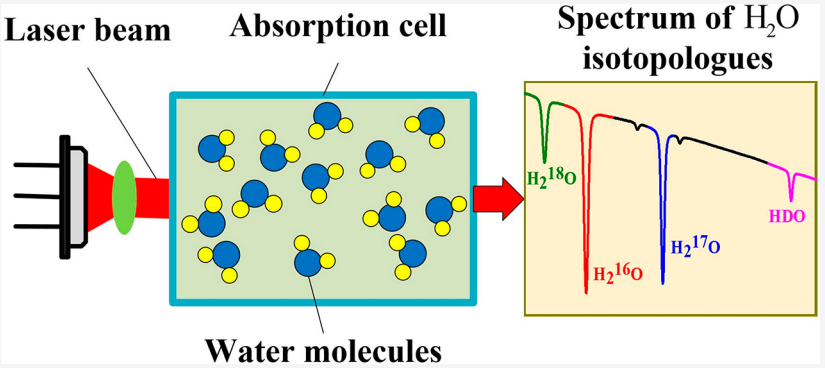

ABSTRACT: A compact isotope ratio sensor based on laser absorption spectroscopy at 2.7 μm was developed for high precision and simultaneous measurements of the D/H, $^{18}O/^{16}O$ and $^{17}O/^{16}O$ isotope ratios in glacier water. Measurements of the oxygen and hydrogen isotope ratios in glacier water demonstrate a 1σ precision of 0.3‰ for $\delta^{18}O$, 0.2‰ for $\delta^{17}O$, and 0.5‰ for $\delta^{2}H$, respectively. The δ values of the working standard glacier water obtained by the calibrated sensor system is basically identical to the IRMS measurement results with a very high calibration accuracy from 0.17‰ to 0.75‰. Preliminary results on the reproducibility measurements display a standard deviation of 0.13‰ for $\delta^{18}O$, 0.13‰ for $\delta^{17}O$, and 0.64‰ for $\delta^{2}H$, respectively.

The study of water isotopes (in the vapor or liquid phase) is applied to a growing number of fields, including atmospheric research, ecology and geochemistry, biomedicine, climate and paleoclimate studies, geological surveys, hydrological studies, and clinical research for diagnosis.[1−11] Particularly, stable isotope is an important target in the study of ice core, since the study of stable isotope of glacier water may be able to date the ice core. Furthermore, water sources of plants, differentiation of evapotranspiration components, isotopic composition of water in mineral water, fruit juice, wine, and liquor are also of great relevance to the isotopic study of water.[12−14]

Isotope ratio mass spectrometry (IRMS) has always been the main technology used by scientific researchers to analyze the isotope ratio with a very high precision from 0.01‰ to 0.1‰ and throughput.[15] But the IRMS instrument is cumbersome, expensive, and usually requires a trained technician for its operation. Particularly, owing to the nature of condensation, the water samples cannot be analyzed directly by the IRMS instrument. Usually, the water samples need to be chemically converted to more easily analyzed gases, such as H_2 and CO_2, to determine the isotope ratios of ^{2}H and ^{18}O.[16] These chemical pretreatments are sometimes hazardous and always time-consuming, which limit the ultimate precision and accuracy, as well as real-time field measurements in most studies. Additionally, isotope ratio measurements of ^{17}O are almost impossible, due to the mass overlap of $^{17}O^{12}C^{16}O$ and $^{16}O^{13}C^{16}O$ molecules.[17] Up to now, no reliable high precision mass spectrometry is available for direct isotope ratio analysis of water samples.

As a strong contestant to IRMS, optical techniques are frequently employed to determine the stable isotope abundance ratios and have attracted a growing interest in recent years.[16−24] At present, isotope ratio laser spectrometry (IRLS) has been widely recognized as a powerful tool to perform in situ and real-time continuous measurements of the stable isotope ratios without requiring chemical conversion in a large variety of environments. Water isotope analyzers based

Received: December 17, 2019
Accepted: February 21, 2020
Published: February 21, 2020

on IRLS have been developed.[17,21,25−29] High precision and high sensitivity IRLS instruments based on OA-ICOS (off-axis integrated cavity output spectroscopy) and CRDS (cavity ring down spectroscopy) methods are now commercially available from LGR Inc. (Los Gatos Research, CA)[30−32] and Picarro Inc. (Santa Clara, CA) to implement the measurements of the stable isotope ratios.[33−36] However, these two products are expensive for some scientific researchers.

In this paper, a compact IRLS instrument using direct absorption spectroscopy was developed for high precision and accuracy measurements of the D/H, $^{18}O/^{16}O$, and $^{17}O/^{16}O$ isotope ratios in glacier water at 2.7 μm. This system is very suitable for real-time and in situ detection of the water isotope ratios with the advantages of simpler design, lower cost, and smaller size. The most significant advantage is that it can realize the direct and simultaneous measurements of isotope ratios of the water samples, especially the direct analysis of ^{17}O, avoiding the time-consuming chemical conversion of the samples that are IRMS required. The isotope ratios can be easily calculated with high sensitivity and precision when temperature, pressure, optical path length, and absorption line strengths of gases are certain. The distributed feedback (DFB) laser was selected in the current work. The advantages of using DFB laser are better mode stability, room temperature operation, smaller size, and cheaper price than the color center laser previously reported.[21]

The experimental spectrum of water isotopologues ($H_2{}^{18}O$, $H_2{}^{16}O$, $H_2{}^{17}O$, and HDO) in the gas phase near 3663 cm^{-1} is very suitable for in situ analysis of these isotopes in liquid water as well as in water vapor in the atmosphere. Measurements of the oxygen and hydrogen isotope ratios in glacier water show a 1σ precision better than those achieved in previous experiments with a DFB laser at 2.7 μm. The calibrated δ values of the working standard glacier water is in accordance with the IRMS measurement results and show a very high accuracy. Preliminary tests of the reproducibility upon injection of fresh samples revealed that $\delta^{18}O$, $\delta^{17}O$, and $\delta^{2}H$ measurements could be carried out with a systematic standard deviation smaller than 0.7‰.

EXPERIMENTAL SETUP

The experimental system used for water isotope ratio measurements is displayed in Figure 1. The light source is a continuous wave room temperature single mode DFB laser at 2.7 μm (nanoplus GmbH) with a tuning range of 4 cm^{-1} and an output power of 2 mW. Table 1 gives the parameters of the four water isotopologues ($H_2{}^{18}O$, $H_2{}^{16}O$, $H_2{}^{17}O$, and HDO) absorption lines selected in the present work. Their positions are from 3662.9196 to 3663.8419 cm^{-1}, totally within the tuning range of the DFB laser. The tuning rates of the DFB laser are 0.05 nm/mA and 0.25 nm/K, respectively, with a line width of smaller than 10 MHz and a side-mode suppression of more than 30 dB.

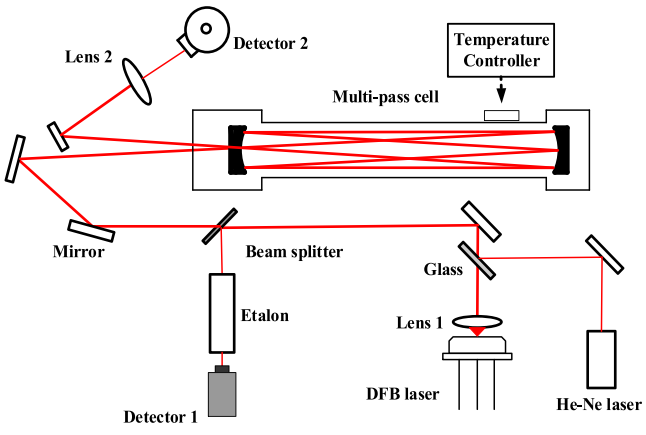

Figure 1. Experimental setup used for water isotope ratio measurements.

The laser beam from the DFB laser was collimated first by a lens with a short focal length of 2.5 mm and then transformed into a quasi-parallel beam. As the mid-infrared light is not visible to human eyes, the alignment of the optical components is aided by a visible He−Ne laser beam which was adjusted to be coaxial with the DFB laser beams. A part of the laser beam was coupled to a homemade Fabry−Perot etalon (free spectral range (FSR) = 0.03225 cm^{-1}) for frequency metrology using a beamsplitter and received by the detector 1 (Vigo detector, PVMI-10.6). The main laser beam was directed to a multipass absorption cell with an optical path length of 100 m. The emerging absorption signal from the cell was focused by a lens onto the detector 2 (J15D22-M204-S01M-60). The detector 2 output was sampled with a fast data acquisition card and then transferred to a personal computer for further data processing and analysis.

The precision of the isotope ratio is very sensitive to temperature changes. Temperature of the multipass absorption cell in our isotope ratio determination experiments was maintained at 30 °C (within ±0.1 °C) by a temperature controller in order to avoid deposit of aqueous water on the optical absorption cell wall (especially on the cell mirrors) and decrease the systematic deviations caused by the temperature changes in the water vapor sample.

PRINCIPLE OF WATER ISOTOPE RATIOS MEASUREMENTS

Based upon the Beer−Lambert law, the integrated absorbance $A(\nu)$ at frequency ν can be expressed as

$$A_I = \int A(\nu)\mathrm{d}\nu = \int \ln(I_0(\nu)/I(\nu))\mathrm{d}\nu = CL\int \sigma(\nu)\mathrm{d}\nu = CLS(T)/n \quad (1)$$

Where $I(\nu)$ and $I_0(\nu)$ are the transmitted and incident probing light intensity, respectively, C (molecules/cm^3) is the number density of the absorbing molecules, $\sigma(\nu)$ (cm^2/ molecule) is the frequency-dependent absorption cross section, and L (cm) is the optical absorption path length. $S(T)$ (cm^{-1}/(mol·cm^{-2})) is the temperature-dependent molecular line absorption intensity, n is the isotope abundance, both can be found in the HITRAN database.

The temperature coefficients were calculated from the ground state energies E' using the following formula:

$$S(T) = S(T_0)\left(\frac{T_0}{T}\right)^{3/2}\exp\left[-hc\frac{E'}{k}\left(\frac{1}{T}-\frac{1}{T_0}\right)\right] \quad (2)$$

with T_0 = 296 K, E_0 (cm^{-1}) is the lower level energy, h (J s) is the Planck constant, c (cm/s) is the speed of light in vacuum, and k (J/K) is the Boltzmann constant. Table 1 lists the temperature coefficients of the ro-vibrational transitions used in this study. A thermal drift of 1 K would lead to a relative change in the line strength of +1.5‰, +4.6‰, −1.4‰, −3.4‰ for the selected absorption lines of $H^{18}OH$, $H^{16}OH$, $H^{17}OH$, and HOD, respectively.

https://dx.doi.org/10.1021/acs.analchem.9b05679
Anal. Chem. 2020, 92, 4512−4517

Table 1. List of the Absorption Lines Parameters Used in This Work[a]

isotopomer	frequency (cm^{-1})	intensity (10^{-23} $cm \cdot mol^{-1}$)	rotational assignment	ground state energy (cm^{-1})	temperature coefficient at 296 K (K^{-1})
$H^{18}OH$	3662.9196	2.1	$5_{15} \leftarrow 5_{14}$	398.4	1.5‰
$H^{16}OH$	3663.0452	8.5	$6_{24} \leftarrow 7_{17}$	586.5	4.6‰
$H^{17}OH$	3663.3213	7.2	$3_{13} \leftarrow 4_{14}$	224.3	−1.4‰
HDO	3663.8419	1.2	$2_{12} \leftarrow 3_{13}$	100.4	−3.4‰

[a]Line positions and assignments were taken from the Hitran2008 database.

The isotope ratio can be obtained using the ratio of the integrated areas A_I and the absorption line intensities S of the isotopic components:

$$R_s = [C^x]/[C^a] = \frac{A_I^x}{A_I^a} \times \frac{S^a/n^a}{S^x/n^x} \quad (3)$$

where x represents the rare isotopic species ($H_2{}^{17}O$, $H_2{}^{18}O$, or HDO), a is the abundant isotopic component ($H_2{}^{16}O$), and R represents the ratio of the rare to the abundant isotopic abundances.

The relative deviation of the isotope ratio in water with respect to the international standard reference known as Vienna Standard Mean Ocean Water (VSMOW), is expressed in terms of the δ-value:

$$\delta(‰) = \frac{R_s - R_{VSMOW}}{R_{VSMOW}} \times 1000 \quad (4)$$

where, R_{vsmow} = 0.0020052 for ^{18}O, 0.0003799 for ^{17}O and 0.00015576 for ^{2}H, respectively. It is noted that eqs 3 and 4 are applied under the conditions of the sample and reference spectra recorded at the same temperature.

Theoretically, with knowledge of the absorption line intensities (provided by HITRAN 2008 database, for instance), the integrated areas can be used to determine the isotopic δ value with respect to the water isotopic composition of the international standard material known as VSMOW. Unfortunately, the absorption line intensity of the molecule is usually not accurate enough for isotopic ratio determination with high precision.

Therefore, our isotope spectrometers are calibrated with the known reference standard of δ_{ref} (or R_{ref}),

$$R_s = R_{ref} \frac{A_s^x}{A_s^a} \times \frac{A_{ref}^a}{A_{ref}^x} \quad (5)$$

Here R_s and R_{ref} are the abundance ratios of samples and reference standards, A_s and A_{ref} are the integrated areas of samples and reference standards, respectively. The δ values of the glacier water working standard DO2 used in the present work were determined by repeated IRMS analysis in the Department of Analytical, Environmental and Geo-Chemistry (AMGC), Université Libre de Bruxelles, Brussels, Belgium. Another glacier water working standard DO3 with different isotopic composition was used to check and evaluate the accuracy of the laser instrument. Table 2 lists the corresponding δ values of the glacier water working standards obtained by means of IRMS. As the IRMS method could not detect the $\delta^{17}O$ directly in water, these values of $\delta^{17}O$ were obtained based on a natural relation between the ^{17}O and ^{18}O abundance ratios: $\delta^{17}O = (1 + \delta^{18}O)^{\lambda} - 1$ with λ = 0.5281.[21] The melted glacier water from the Antarctic Pole was used as the unknown sample material.

Table 2. δ Values of the Glacier Water Working Standards Determined by IRMS

label	$\delta^{18}O$	$\delta^{17}O$	$\delta^{2}H$
DO3	−22.307‰	−11.843‰	−127.306‰
DO2	−7.789‰	−4.120‰	−45.434‰

RESULTS AND DISCUSSION

One of the most important aspects in water isotopic ratio measurements is the choice of appropriate absorption lines, which has a direct impact on the measurement sensitivity and precision. The parameters of the absorption lines used in this work are listed in Table 1. It is very clear that the used four absorption lines have similar absorption depths at natural abundance with an absorption intensity up to 10^{-23} $cm \cdot mol^{-1}$. In favor of minimizing the effects of temperature-dependent line intensities, these lines should also have similar ground state energy.

Eight μL liquid glacier water samples were injected into the pre-evacuated multipass absorption cell through a silicon membrane using a syringe, resulting in a very low water vapor pressure of 3.5 mbar inside the absorption cell. The saturated vapor pressure is ∼42 mbar, and all injected liquid glacier water quickly evaporates inside the evacuated gas cell. Figure 2 shows the glacier water isotope absorption spectrum recorded in this work. The four absorption lines are free from interferences from the same or other species. These absorption features of the glacier water were fitted to Voigt profiles using labview software in order to determine the integrated area A_I under the absorption lines. During the fitting procedure, the Gaussian width was fixed, and the Lorentzian width was relaxed at the low pressure of 3.5 mbar. The baseline was

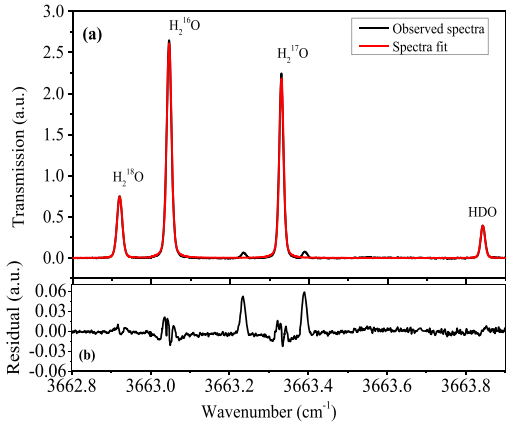

Figure 2. (a) Experimental spectra observed in this work (black lines) and the corresponding Voigt fitting spectra (red lines). (b) Fitting residuals. The two minor black absorption peaks not fitted are HDO absorption lines which are not used to do analysis of the stable isotope ratios in this study.

https://dx.doi.org/10.1021/acs.analchem.9b05679
Anal. Chem. 2020, 92, 4512−4517

modeled with a fourth-order polynomial to account for the laser intensity ramp.

In order to assess the best stable time of the system, raw measured δ values with a 1 s time interval were used to perform the Allan variance analysis and displayed in Figure 3a.

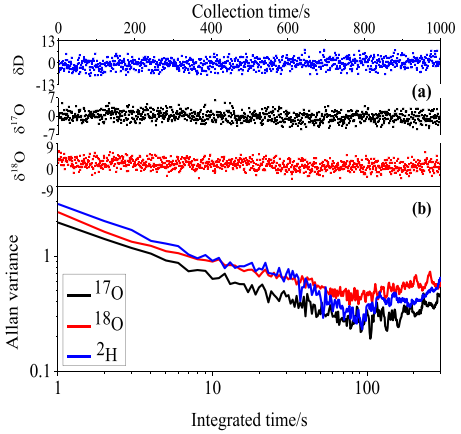

Figure 3. (a) Raw measurements of $\delta^{18}O$, $\delta^{17}O$, and $\delta^{2}H$ with 1 s acquisition time. (b) The Allan variance with an optimal averaging time of about 100 s for the present laser system. $\delta^{18}O$, $\delta^{17}O$, and $\delta^{2}H$ are shown in red, black, and blue, respectively.

In the present work, the raw measured δ values with 1 s precision were 2.0‰ for $\delta^{18}O$, 1.7‰ for $\delta^{17}O$, and 2.8‰ for $\delta^{2}H$, respectively. The optimal averaging time for the present sensor was ∼100 s and shown in Figure 3b. Thus the optimal averaging time of 100 s was used to analyze the performance and precision of the system.

Figure 4 displays the short-term reproducibility of $\delta^{18}O$, $\delta^{17}O$, and $\delta^{2}H$. As each measurement took 100 s, the total

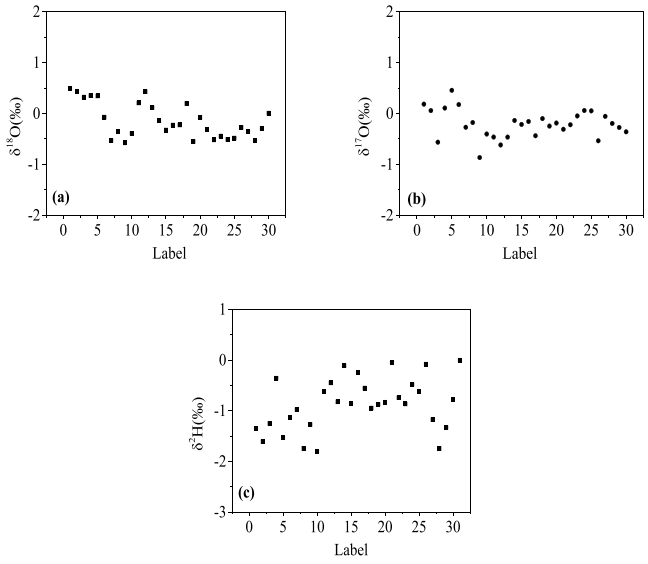

Figure 4. Short-term reproducibility results of (a) $\delta^{18}O$, (b) $\delta^{17}O$, and (c) $\delta^{2}H$ with a single measurement time of 100 s.

acquisition time was equal to 50 min for series of 30 measurements. Of these, measurement results that more than 3 times the absolute deviation from the median were removed from the figure and excluded from further statistical analysis. Accordingly, between 5% and 10% of the measurement results in a typical experiment were considered to be outliers. Moreover, the results of the first three injections were abandoned for each isotope ratio determination to avoid the sample memory effects due to the "stickness" of glacier water on the wall of the absorption cell. The improved 1 σ precision was 0.3‰ for $\delta^{18}O$, 0.2‰ for $\delta^{17}O$, and 0.5‰ for $\delta^{2}H$, respectively.

The line strengths from the Hitran database are usually not accurate for isotopic ratio determination with high precision. For this reason, the glacier water reference standard DO3 listed in Table 2 was used to calibrate the system. The ratio of A^{a}_{ref}/A^{x}_{ref} in eq 5 was obtained from the average value of the measurements of three independent injection of glacier water standard DO3. The accuracy of the sensor system was evaluated by measuring another glacier water reference standard DO2 ($\delta^{18}O$ = −7.789‰, $\delta^{17}O$ = −4.12‰, and $\delta^{2}H$ = −45.434‰), which was very different from DO3. Table 3 shows the measurement results of both IRMS and our IRLS sensor. It can be seen that the δ values obtained by our IRLS sensor is in agreement with the IRMS measurement results.

Table 3. Measurement Results of DO2 from IRMS and our IRLS System

	$\delta^{18}O$(SD)	$\delta^{17}O$(SD)	$\delta^{2}H$(SD)
IRMS	−7.789‰	−4.120‰	−45.434‰
IRLS sensor	−7.858‰	−4.157‰	−45.467‰

We also checked the reproducibility of the three isotopomers over several days through different series of measurements, each time filling the absorption cell with 8 μL of the same melted glacier water sample, followed by evacuation, flushing, and refilling, before starting a new series. Over a time interval of 6 days, we found mean values ranging from −8.092‰ to −7.689‰ for the $\delta^{18}O$ of DO2, with an overall average value of −7.858‰ and a standard deviation (1σ) of 0.13‰. The values for the $\delta^{17}O$ and $\delta^{2}H$ were found in the range of −4.371‰ to −3.961‰, and −46.216‰ to −44.716‰ with overall average values of −4.157‰ and −45.467‰ and 1σ standard deviation of 0.13‰ and 0.64‰, respectively. This test also provides preliminary information on the level of accuracy. The calibration accuracy of the δ values is about from 0.17‰ to 0.75‰. Although the unequal average δ values indicate the presence of a systematic deviation, the average $\delta^{18}O$, $\delta^{17}O$, and $\delta^{2}H$ values were well within the long term precision level. The results of the long-term reproducibility tests are presented in Table 4.

The causes of the apparent δ shifts need to be found out and discussed. We consider that these apparent δ shifts are not due to instability of the temperature control of the system. The molecular absorption line strength is related to the temperature, which can be found in eq 2. Temperature changes of the absorption cell may cause system deviation in the isotope ratio determinations. Particularly, using the temperature coefficients of the four absorption lines reported in Table 1, we may obtain the shifts in $\delta^{18}O$, $\delta^{17}O$, and $\delta^{2}H$ are about 3.1‰/K, 6.0‰/K, and 8.0‰/K, respectively. The observed fluctuations in the $\delta^{2}H$ value indicate a temperature difference of 0.19 K through the whole measurement time of 6 days. But this temperature differences should lead to much smaller variations in the $\delta^{18}O$ and $\delta^{17}O$ values than the $\delta^{2}H$, which are listed in Table 4. Becasue they have smaller temperature coefficients than $\delta^{2}H$. The temperature of the used absorption cell in our experiment

https://dx.doi.org/10.1021/acs.analchem.9b05679
Anal. Chem. 2020, 92, 4512−4517

Table 4. Results of the Long-Term Reproducibility of $\delta^{18}O$, $\delta^{17}O$ and $\delta^{2}H$

date	mean $\delta^{18}O$ value (‰)	$\delta^{18}O$ standard deviation (‰)	mean $\delta^{17}O$ value (‰)	$\delta^{17}O$ standard deviation (‰)	mean $\delta^{2}H$ value (‰)	$\delta^{2}H$ standard deviation (‰)
June 28	−7.697	0.31	−4.062	0.22	−44.819	0.53
June 29	−7.689	0.27	−4.168	0.19	−45.338	0.44
June 30	−7.787	0.38	−4.212	0.18	−45.515	0.47
June 30	−7.959	0.33	−4.371	0.21	−46.216	0.52
July 1	−8.092	0.24	−3.968	0.21	−46.119	0.51
July 2	−7.867	0.32	−3.961	0.19	−44.839	0.60
July 2	−7.891	0.36	−4.209	0.25	−44.716	0.54
July 2	−7.794	0.27	−4.164	0.18	−45.816	0.45
July 3	−7.946	0.30	−4.298	0.23	−45.798	0.52

was monitored with a calibrated platinum resistor (Pt100) (with an accuracy of 0.03 °C and a precision of 0.01 °C). No temperature gradient variation along the cell axis has been observed within the measurement precision of the temperature sensors. The sample temperature stabilization was controlled within ±0.1 K to ensure a measurement precision smaller than 1‰.

In our experiment, a slight drift of the DFB laser wavelength with time has been observed. The DFB laser used in this work was temperature controlled by the Laser Diode Controller 501 (Stanford Research Systems). The temperature control accuracy is ±0.01 °C with a long-term stability (24 h) of ±0.002 °C. The slight shift of wavelength will cause the change of line positions and line shapes, thus may affect the determination of A_I in eq 1 and the long-term accuracy of the δ value.

Furthermore, it is difficult to guarantee that the gas pressure in the absorption cell is 3.5 mbar after each injection of glacier water. The differential pressure may influence the accuracy of the sample spectrum fitting. Such pressure differences occur in fact due to our inability to inject 8 μL glacier water samples with an uncertainty smaller than 0.1 μL. As a result, the contributions of some non-Voigt profiles make the line widths in the sample specra different. Line overlapping may be responsible for pressure-dependent asymmetries, further limiting the accuracy of the spectra fitting. An analysis method based on the simultaneous fit of multiple absorption lines would not suffer from such a differential pressure effect. Nevertheless, the spectral overlapping of $H^{17}OH$ absorption lines, clearly in Figure 2, may strengthen the effect of differential pressure on the $\delta^{17}O$ values. In the calculation of the δ values according to eq 4, the line shape change of the spectral caused by the pressure corresponding to the rare isotope would be canceled by the same change in the abundant isotope line shape. A disadvantage of the simultaneous fit to all absorption lines present in the experimental spectrum is the requirement of a proper calibration of the frequency scale. The frequency scale in this work was linearized using the interference fringes of the etalon. Positions of water vapor absorption lines from the HITRAN2008 database provided an absolute frequency reference for frequency calibration. In most cases, the line-by-line, sample spectral fitting procedure is better than the multiple absorption lines fitting method, the premise is that well-calibrated corrections are made for the differential pressure between the different samples. In the following experiments, we need to guarantee the injection capacity with higher accuracy. In the present work, it takes about 10 seconds to reach equilibrium of the pressure after each injection of glacier water, and then during each individual measurement, the pressure can be maintained for about an hour with a precision of 0.1 mbar.

CONCLUSIONS

We have demonstrated that the development of a compact IRLS sensor enables the simultaneous measurements of $^{2}H/^{1}H$, $^{17}O/^{16}O$, $^{18}O/^{16}O$ isotope abundance ratios in glacier water. Preliminary tests of the short and long-term reproducibility upon injection of fresh glacier water samples, performed in different time interval, revealed that $\delta^{18}O$, $\delta^{17}O$, and $\delta^{2}H$ measurements could be carried out with standard deviation smaller than 0.7‰. The δ values of the working standard glacier water obtained by our calibrated sensor system was in agreement with the IRMS measurement results with a very high calibration accuracy from 0.17‰ to 0.75‰. Measurements of the oxygen and hydrogen isotope ratios in glacier water showed a 1σ precision of 0.3‰ for $\delta^{18}O$, 0.2‰ for $\delta^{17}O$, and 0.5‰ for $\delta^{2}H$, respectively. The experimental spectrum of water isotopologues ($H_2{}^{18}O$, $H_2{}^{16}O$, $H_2{}^{17}O$, and HDO) in the gas phase near 3663 cm^{-1} is very suitable for in situ analysis of these isotopologues in liquid water as well as in water vapor in the atmosphere. Overall, IRLS has becomes a feasible choice to conventional IRMS with the advantages of fast and direct measurements on water samples, no sample pretreatment, smaller size, lower cost, and high precision.

AUTHOR INFORMATION

Corresponding Author

Xiaojuan Cui − *Anhui Provincial Key Laboratory of Photonic Devices and Materials, Anhui Institute of Optics and Fine Mechanics, Chinese Academy of Sciences, Hefei 230031, China;* orcid.org/0000-0003-2850-377X; Email: cuixiaojuan@aiofm.ac.cn

Authors

Weidong Chen − *Laboratoire de Physicochimie de l'Atmosphère, Université du Littoral Côte d'Opale, 59140 Dunkerque, France*

Markus Werner Sigrist − *ETH Zurich, Institute for Quantum Electronics, CH-8093 Zurich, Switzerland*

Eric Fertein − *Laboratoire de Physicochimie de l'Atmosphère, Université du Littoral Côte d'Opale, 59140 Dunkerque, France*

Pascal Flament − *Laboratoire de Physicochimie de l'Atmosphère, Université du Littoral Côte d'Opale, 59140 Dunkerque, France*

Kevin De Bondt − *Department of Analytical, Environmental and Geo-Chemistry (AMGC), Université Libre de Bruxelles, Brussels, Belgium*

Nadine Mattielli − *Department of Analytical, Environmental and Geo-Chemistry (AMGC), Université Libre de Bruxelles, Brussels, Belgium*

https://dx.doi.org/10.1021/acs.analchem.9b05679
Anal. Chem. 2020, 92, 4512−4517

Complete contact information is available at:
https://pubs.acs.org/10.1021/acs.analchem.9b05679

Notes

The authors declare no competing financial interest.

■ ACKNOWLEDGMENTS

This work is partly supported by National Natural Science Foundation of China (Grant No. 41775128, 11204319), the Special Fund for Basic Research on Scientific Instruments of the Chinese Academy of Science (Grant No. YZ201315) and the Chinese Academy of Science President's International Fellowship Initiative (PIFI, 2015VMA007). Finally, the Scientific Research Foundation for the Returned Overseas Chinese Scholars, State Education Ministry, is gratefully acknowledged.

■ REFERENCES

(1) Webster, C. R.; Heymsfield, A. J. *Science* **2003**, *302*, 1742−1745.
(2) Landais, A.; Masson-Delmotte, V.; Stenni, B.; Selmo, E.; Roche, D. M.; Jouzel, J.; Lambert, F.; Guillevic, M.; Bazin, L.; Arzel, O.; Vinther, B.; Gkinis, V.; Popp, T. *Quat. Sci. Rev.* **2015**, *114*, 18−32.
(3) Sturm, C.; Zhang, Q.; Noone, D. *Clim. Past* **2010**, *6*, 115−129.
(4) Uchiyama, R.; Okochi, H.; Ogata, H.; Katsumi, N.; Asai, D.; Nakano, T. *Atmos. Res.* **2017**, *194*, 109−118.
(5) Shao, L.; Tian, L.; Cai, Z.; Cui, J.; Zhu, D.; Chen, Y.; Palcsuf, L. *Atmos. Res.* **2017**, *188*, 48−54.
(6) Baer, T.; Barbour, S. L.; Gibson, J. J. *J. Hydrol.* **2016**, *541*, 1155−1164.
(7) Yang, C.; Yang, S.; Su, N. *Chem. Geol.* **2016**, *441*, 14−23.
(8) Rangarajan, R.; Laskar, A. H.; Bhattacharya, S. K.; Shen, C.; Liang, M. *J. Hydrol.* **2017**, *547*, 111−123.
(9) Hatvani, I. G.; Leuenberger, M.; Kohan, B.; Kern, Z. *Polar Sci.* **2017**, *13*, 23−32.
(10) Affolter, S.; Hauselmann, A. D.; Fleitmann, D.; Hauselmann, P.; Leuenberger, M. *Quat. Sci. Rev.* **2015**, *127*, 73−89.
(11) Matthews, D. E. *JPEN, J. Parenter. Enteral Nutr.* **1991**, *15*, 691−692.
(12) Rosenlof, K. H. *Science* **2003**, *302*, 1691−1692.
(13) Moyer, E.; Irion, F.; Yung, Y.; Gunson, M. *Geophys. Res. Lett.* **1996**, *23*, 2385−2388.
(14) Dessler, A. E.; Sherwood, S. C. *Atmos. Chem. Phys.* **2003**, *3*, 2173−2181.
(15) Hofstetter, D.; Francesco, J. D.; Hvozdara, L.; Herzig, H. P.; Beck, M. *Appl. Phys. B: Lasers Opt.* **2011**, *103*, 967−970.
(16) Kerstel, E.; Gianfrani, L. *Appl. Phys. B: Lasers Opt.* **2008**, *92*, 439−449.
(17) Gianfrani, L.; Gagliardi, G.; Burgel, M.; Kerstel, E. R. Th. *Opt. Express* **2003**, *11*, 1566−1576.
(18) Bartlome, R.; Sigrist, M. W. *Opt. Lett.* **2009**, *34*, 866−868.
(19) Richter, D.; Wert, B. P.; Fried, A.; Weibring, P.; Walega, J. G.; White, J. W. C.; Vaughn, B. H.; Tittel, F. K. *Opt. Lett.* **2009**, *34*, 172−174.
(20) Joly, L.; Parvitte, B.; Zéninari, V.; Courtois, D.; Durry, G. *J. Quant. Spectrosc. Radiat. Transfer* **2006**, *102*, 129−138.
(21) Kerstel, E. R. Th.; Trigt, R.; Dam, N.; Reuss, J.; Meijer, H. A. J. *Anal. Chem.* **1999**, *71*, 5297−5303.
(22) Wu, T.; Chen, W.; Kerstel, E.; Fertein, E.; Masselin, P.; Gao, X.; Zhang, W.; Wang, Y.; Koeth, J.; Bruckner, D.; He, X. *Sensors* **2014**, *14*, 9027−9045.
(23) Joly, L.; Zéninari, V.; Parvitte, B.; Courtois, D. *Opt. Lett.* **2006**, *31*, 143−145.
(24) Kerstel, E. R. T.; Iannone, R. Q.; Chenevier, M.; Kassi, S.; Jost, H. J.; Romanini, D. *Appl. Phys. B: Lasers Opt.* **2006**, *85*, 397−406.
(25) Kerstel, E.R. Th.; Gagliardi, G.; Gianfrani, L.; Meijer, H. A. J.; Trigt, R.; Ramaker, R. *Spectrochim. Acta, Part A* **2002**, *58*, 2389−2396.
(26) Nadezhdinsky, A. I.; Ponurovsky, Ya. Ya.; Shapovalov, Y. P.; Popov, I. P.; Stavrovsky, D. B.; Khattatov, V. U.; Galaktionov, V. V.; Kuzmichev, A. S. *Appl. Phys. B: Lasers Opt.* **2012**, *109*, 505−510.
(27) Dyroff, C.; Fütterer, D.; Zahn, A. *Appl. Phys. B: Lasers Opt.* **2010**, *98*, 537−548.
(28) Sayres, D. S.; Moyer, E. J.; Hanisco, T. F.; St. Clair, J. M.; Keutsch, F. N.; O'Brien, A.; Allen, N. T.; Lapson, L.; Demusz, J. N.; Rivero, M. *Rev. Sci. Instrum.* **2009**, *80*, 044102.
(29) Iannone, R. Q.; Romanini, D.; Cattani, O.; Meijer, H. A. J.; Kerstel, E.R. Th. *J. Geophys. Res.* **2010**, *115*, 10111−10123.
(30) Soulsby, C.; Birkel, C.; Tetzlaff, D. *Geophys. Res. Lett.* **2014**, *41*, 442−448.
(31) Berman, E. S. F.; Levin, N. E.; Landais, A.; Li, S.; Owano, T. *Anal. Chem.* **2013**, *85*, 10392−10398.
(32) Kurita, N.; Newman, B. D.; Araguas-Araguas, L. J.; Aggarwal, P. *Atmos. Meas. Tech.* **2012**, *5*, 2069−2080.
(33) Gupta, P.; Noone, D.; Galewsky, J.; Sweeney, C.; Vaughn, B. H. *Rapid Commun. Mass Spectrom.* **2009**, *23*, 2534−2542.
(34) Arienzo, M. M.; Swart, P. K.; Vonhof, H. B. *Rapid Commun. Mass Spectrom.* **2013**, *27*, 2616−2624.
(35) Steig, E. J.; Gkinis, V.; Schauer, A. J.; Schoenemann, S. W.; Samek, K.; Hoffnagle, J.; Dennis, K. J.; Tan, S. M. *Atmos. Meas. Technol. Discuss.* **2013**, *6*, 10191−10229.
(36) Godoy, J. M.; Godoy, M. L. D. P.; Neto, A. *J. Geochem. Explor.* **2012**, *119*−*120*, 1−5.